ISSN: 2278 – 7798
International Journal of Science, Engineering and Technology Research (IJSETR)
Volume 5, Issue 7, July 2016

Experimental Investigation on the Supercavitating Flows over a Cylindrical Body with Conical Cavitators

Vahid Farhangmehr, Mohammad Hossein Dashti

***Abstract*—In this study, the supercavitating flows with the variable velocities in an open-circuit water tunnel over a cylindrical underwater body equipped with a cavitator are investigated experimentally. The cavitators are cones with the angles of 30°, 45°, 60°, and a flat disk. In order to analyze the dynamic behavior of supercavity and derive its geometrical characteristics e.g., its length and diameter, a high-speed photography system is employed. Besides, several convenient sensors are used to measure the pressure distribution along the body and the drag force. To validate the experiments, the results obtained for the case of disk-shaped cavitator are compared with the available information in the literature. Also the effects of air injection into the supercavity on its interaction with the body are considered. The results of present study can be employed in design and optimization of the shape and the hydrodynamic performance of the cavitators in the underwater vehicles.**

***Index Terms*—air injection, cylindrical body, cavitator, open-circuit water tunnel, supercavity**

[1] INTRODUCTION

Increase in velocity and the range of underwater vehicles, e.g., submarines, with considerable decrease in the skin friction drag on their surfaces has been an attractive research topic. When a body with an attached nose or cavitator moves in the water with an appropriate velocity, a cavity containing gas, vapor or a mixture of both is formed behind the nose or cavitator and develops with decrease in the cavitation number. This cavity in the form of a supercavity can surround the whole or the major part of body and so cause the water not to contact it. Thus, the skin friction drag will be negligible and only restricted to the nose or cavitator. In order to decrease the cavitation number to achieve a supercavity with a great length and consequently, a small skin friction drag, the hydrodynamic pressure should be decreased. This is feasible by providing a high initial velocity for the body. As an alternative to this high initial velocity, the air injection into the supercavity can be used in order to keep the body inside it. In this case, the geometrical characteristics of supercavity such as its diameter and length will depend on the volumetric flow rate of injected air, the velocity of body and the geometrical shape of the nose or cavitator.

There are numerous experimental, numerical and analytical investigations on the supercavitation in the literature [1], [2], [3]. A supercavitating body during its motion in shallow waters experiences a blockage effect which influences both the length and diameter of supercavity. When the cavitation number of flow is below the cavitation number of blockage, the supercavity length tends to become infinite. Based on the ideal fluid theory, Amromin [4] showed that the influences of boundaries in the shallow waters lead to three-dimensional deformations in the supercavity profile and also affect the hydrodynamic performance of the body. The utilization of cavitators can decrease the energy consumption in the high-speed underwater vehicles. Thus, Shafaghat *et al.* [5]-[6]-[7] studied the shape optimization of two-dimensional symmetric and axisymmetric cavitators in two-dimensional symmetric and axisymmetric supercavitating potential flows applying a multi-objective optimization algorithm besides the boundary element method. Hu *et al.* [8] developed the Dispersion-Controlled Dissipative (DCD) scheme for the numerical simulation of the supercavitating flows based on the Lax–Friedrichs numerical flux splitting method. Park and Rhee [9] studied numerically the high-speed supercavitating flows over the two-dimensional symmetric wedge-shaped cavitators by employing the finite-volume method based on the unsteady Reynolds-Averaged Navier–Stokes (RANS) equations. Comparing computed geometrical characteristics of supercavity and the dynamic characteristics of flow to available analytical, numerical and experimental information showed fairly a good agreement. Roohi *et al.* [10] simulated the supercavitating flows over a hydrofoil by applying the finite-volume method which is profiting from the Large Eddy Simulation (LES) turbulence model, the Kunz and Sauer mass transfer models and the Volume of Fluid (VOF) technique for the numerically capturing the boundary of supercavity. They compared the results with the available experimental data and found that the combination of LES, VOF and Kunz model is efficient to simulate the dynamic behavior of the supercavity accurately. Shang [11] conducted a numerical research on the supercavitating flows over the submarines by k–ω SST turbulence model accompanying with VOF technique and the Sauer mass transfer model within the broad range of the cavitation numbers. Saranjam [12] studied the geometrical and dynamic characteristics of supercavitating flows over an underwater body both experimentally by using a high-speed camera and numerically by employing the unsteady RANS equations. Experimental and numerical results showed a good agreement in his work. Pendar and Roohi [13] investigated

***Manuscript received July, 2016*.**

***Vahid Farhangmehr**, Faculty of Engineering, University of Bonab, Bonab, Iran, +98 9143206735*

***Mohammad Hossein Dashti**, Monenco Iran Consulting Engineers, Tehran, Iran, +98 9122453032.*

numerically on the unsteady supercavitating flows over a three-dimensional hemispherical head-form body and a conical cavitator within a wide range of cavitation numbers applying LES and k-ω SST turbulence models, Kunz and Sauer mass transfer models and VOF technique.

Air injection into the supercavity influences its geometrical characteristics, e.g., its length and diameter and also the hydrodynamics of flow [14], [15], [16], [17], [18]. Zhou *et al.* [19] studied numerically both the steady and unsteady three-dimensional ventilated supercavitating flows around an underwater body. They did their simulations by using the finite-volume method benefiting from the Shear Stress Transport (SST) and Detached Eddy Simulation (DES) turbulence models besides the two-fluid multiphase flow model. Nouri *et al.* [20] explored both the hydrodynamics and hydroacoustics of ventilated supercavitating flows numerically by employing LES turbulence model and the physical source and sink model.

In current research, an experimental investigation on the supercavitating flows at different velocities over a cylindrical body equipped with different conical cavitators of angles 30°, 45°, 60°, and a flat disc-shaped cavitator is conducted by utilizing an open-circuit water tunnel, a high-speed camera besides convenient calibrated measuring instruments and a data-recording system. The results comprise the geometrical characteristics of supercavity such as its length and diameter and also the drag force. By comparing the results for the case of flat disc-shaped cavitator with information available in the literature, the validation of experiments is verified. Moreover, the effects of the air injection into the supercavity on its interaction with the body are studied.

[2] Experimental Setup

In the present work, the experiments have been conducted in an open-circuit water tunnel that a schematic of it has been illustrated in Fig.1. Easiness in its design and construction and also the limited equipment used for it are its important features compared to a closed-circuit water tunnel. In the open-circuit water tunnel, a tank is filled with a definite height of water and is injected with air with an adjustable pressure regarding to flow velocity in the test section. The test section is a cylinder of 20 cm length and 40 mm inner diameter made of very smooth and transparent plexiglass. Fig.2 shows a model consisting of cylindrical body and a conical cavitator inside the test section. To flow of water uniformly into the test section, a ball valve has been employed. The maximum velocity of flow in the test section is 45 m/s. Regarding to decrease in the water height in the tank during the experiments and thus the change of both hydrostatic and air pressures, the velocity of flow in the test section is variable. The minimum flow velocity in the test section is 12 m/s. In all experiments, the distance between the model and the inlet of test section is three times of the test section diameter. In the present study, three conical cavitators of angles 30°, 45°, 60° and also a flat disk-shaped cavitator depicted in Fig.3 have been used.

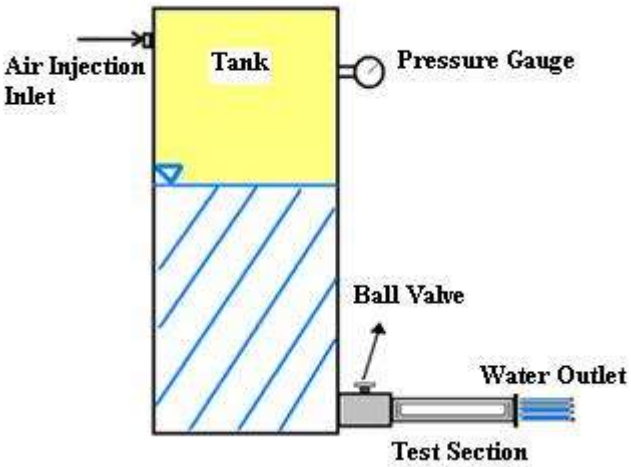

Fig.1. Schematic representation of the open-circuit water tunnel

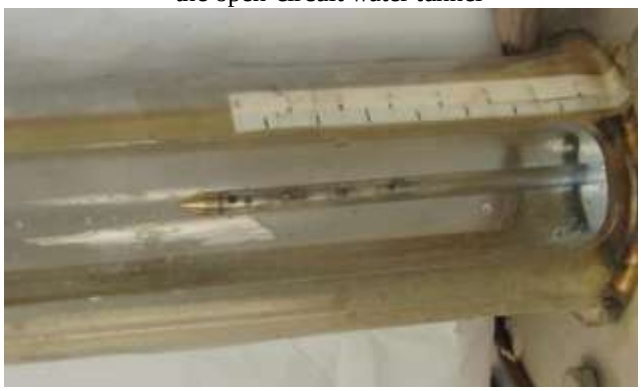

Fig.2. The model comprising of cylindrical body and a conical cavitator inside the test section

Fig.3. Conical and flat disk-shaped cavitators

In Fig.4, the model and the locations of pressure sensors installed on the cylindrical body and the cavitator's tip have been depicted. The distance between the cavitator and the wall of test section is 3.5 times of the base diameter of cavitator which is considered as 5 mm. It is better to mention that these accurate and calibrated sensors do not cause any disorder in the flow.

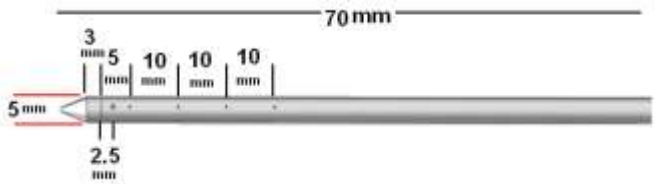

Fig.4. Schematic representation of the geometry of cylindrical body, cavitator and the locations of pressure sensors on the cylindrical body

In order to keep the stability of model and also prevent its vibration, a standard NACA airfoil trimmed at its end has been used such that has the least influences on the outgoing flow from the test section. The sensor of drag force can be placed inside it. This waterproof sensor with diameter of 20 mm has been employed for accurately measuring the sum of pressure and skin friction drag forces. Two views of the inside and outside of the airfoil have been illustrated in Figs.5 and 6.

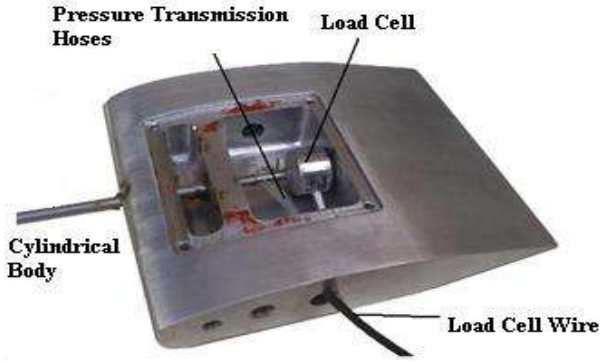

Fig.5. The outside view of trimmed NACA airfoil

Fig.6. The inside view of trimmed NACA airfoil

The important parameter in supercavitating flows is the cavitation number which is defined based on hydrodynamic characteristics of flow as:

Error! Reference source not found. (1)where **Error! Reference source not found.** are the pressure, the pressure inside the supercavity which is the sum of saturated vapor pressure and the partial pressure of the none-condensable gases, and the far-field pressure, respectively [21].

In the case of ventilated supercavitation, to measure the volumetric flow rates of the injected air into the supercavity through four small pores on the body in the vicinity of cavitator's base, a venturi represented in Fig.7 has been used.

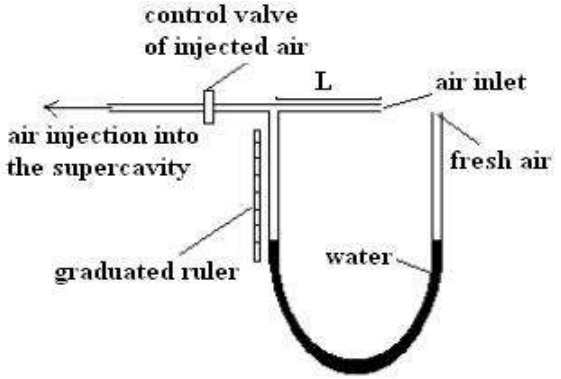

Fig.7. Schematic representation of venturi for measuring the volumetric flow rate of injected air into the supercavity

A high-speed camera (PhantomV12.1 with a filming speed of 20,000 frames per second) with an appropriate illumination has been applied in order to capture the dynamic behavior of supercavity. The water temperature in all experiments is 10°C.

[3] RESULTS AND DISCUSSION

After filling the tank with definite height of water to supply the hydrostatic pressure and then injecting air to its upper part and in the case of ventilated supercavitation, after activating the air injection system into the supercavity, the ball valve is opened to set up the supercavitating flow in the test section. Simultaneously, a high-speed camera is used to capture the dynamic evolution of the supercavity and also extract its geometrical characteristics such as its length and diameter. Other parameters e.g., the tank pressure, pressure distribution along the cylindrical body and the pressure at the cavitator's tip in conjunction with the drag force are measured by convenient calibrated sensors. With adjusting the water height in the tank and the amount of injected air to its upper part, the supercavitating flows with different velocities inside the test section around the model are obtained. The discharged water is collected and returned to tank by a pump. The flow velocity in the test section and the cavitation number are determined by using the pressure at the cavitator's tip and the pressure of test section.

Fig.8 illustrates the gradual decrease in air pressure in the tank, the pressure in the test section and the pressure at the cavitator's tip versus the time. Figs.9 represent the gradual decrease in flow velocity in the test section and consequently, the gradual increase in cavitation number versus the time for conical cavitator of angle 30°, respectively. All these curves are expectable because of gradual decrease in the hydrostatic height of water in the tank.

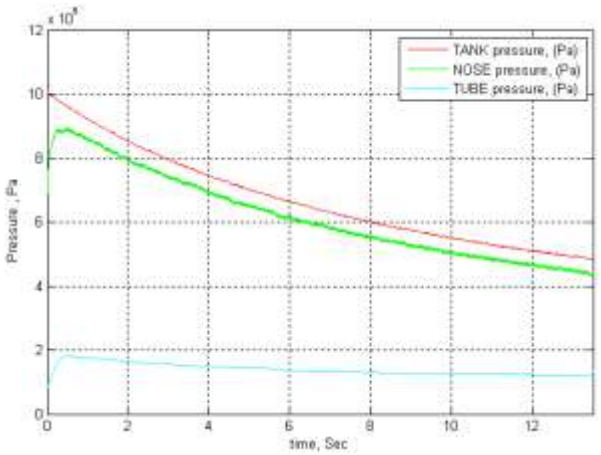

Fig.8. Time-history curves of air pressure in the tank, the pressure in the test section and the pressure at the cavitator's tip for the conical cavitator of angle 30°

In order to validate the experiments, the ratio of the supercavity length to the base diameter of flat dick-shaped cavitator has been compared to the experimental information available in the literature versus the cavitation number in Fig.10. A good agreement is comprehended.

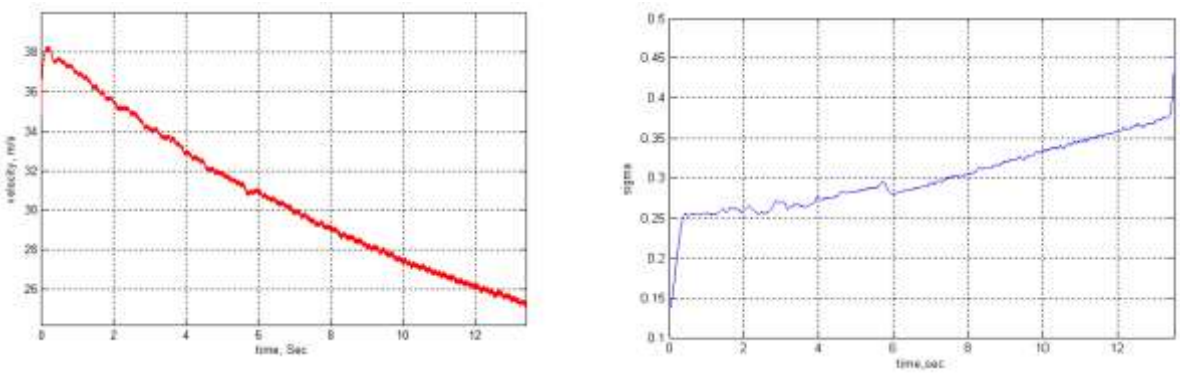

Figs.9. Time-history curve of flow velocity and the cavitation number in the test section for the conical cavitator of angle 30°

Figs.11-12 respectively show the ratio of length and the maximum diameter of supercavity to the base diameter of different cavitators versus the cavitation number. It is seen that increase in the cavitator's angle leads to increase in supercavity length and the flat disk-shaped cavitator results in a supercavity with the greatest length. Additionally, the non-dimensional supercavity diameter increases for conical cavitators with their angle.

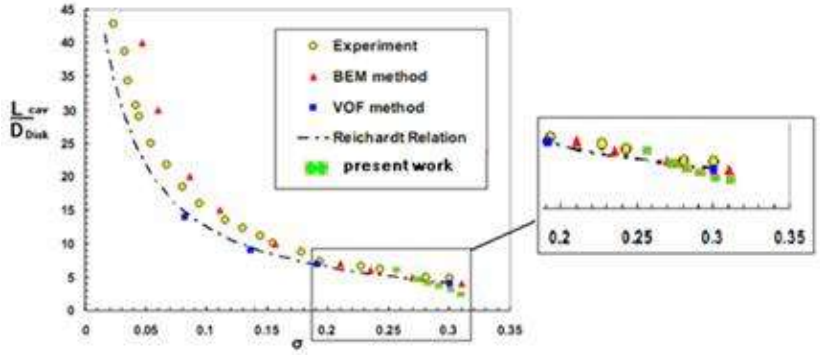

Fig.10. The validation of experiments by comparing the non-dimensional length of supercavity for the case of flat disk-shaped cavitator with the available information [21]

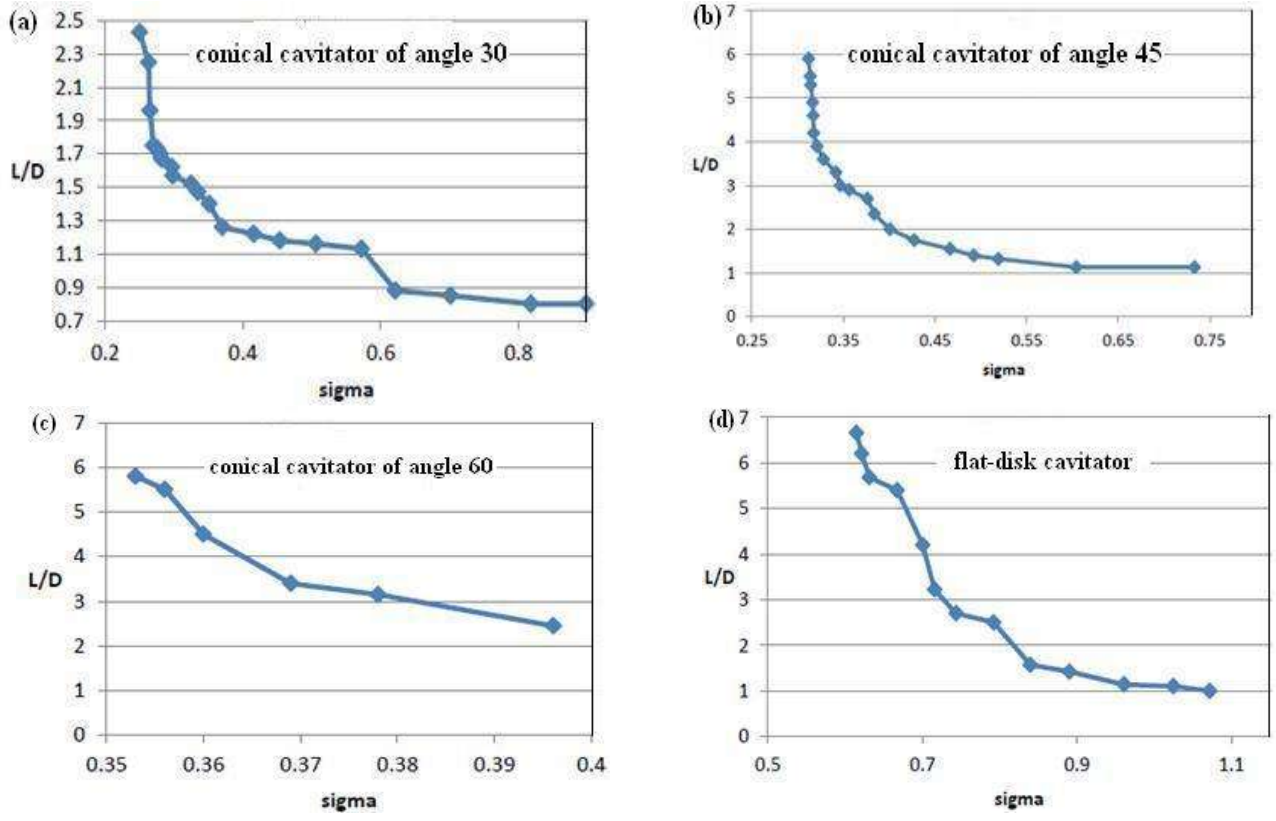

Figs.11. The ratio of supercavity length to the base diameter of different cavitators versus the cavitation number

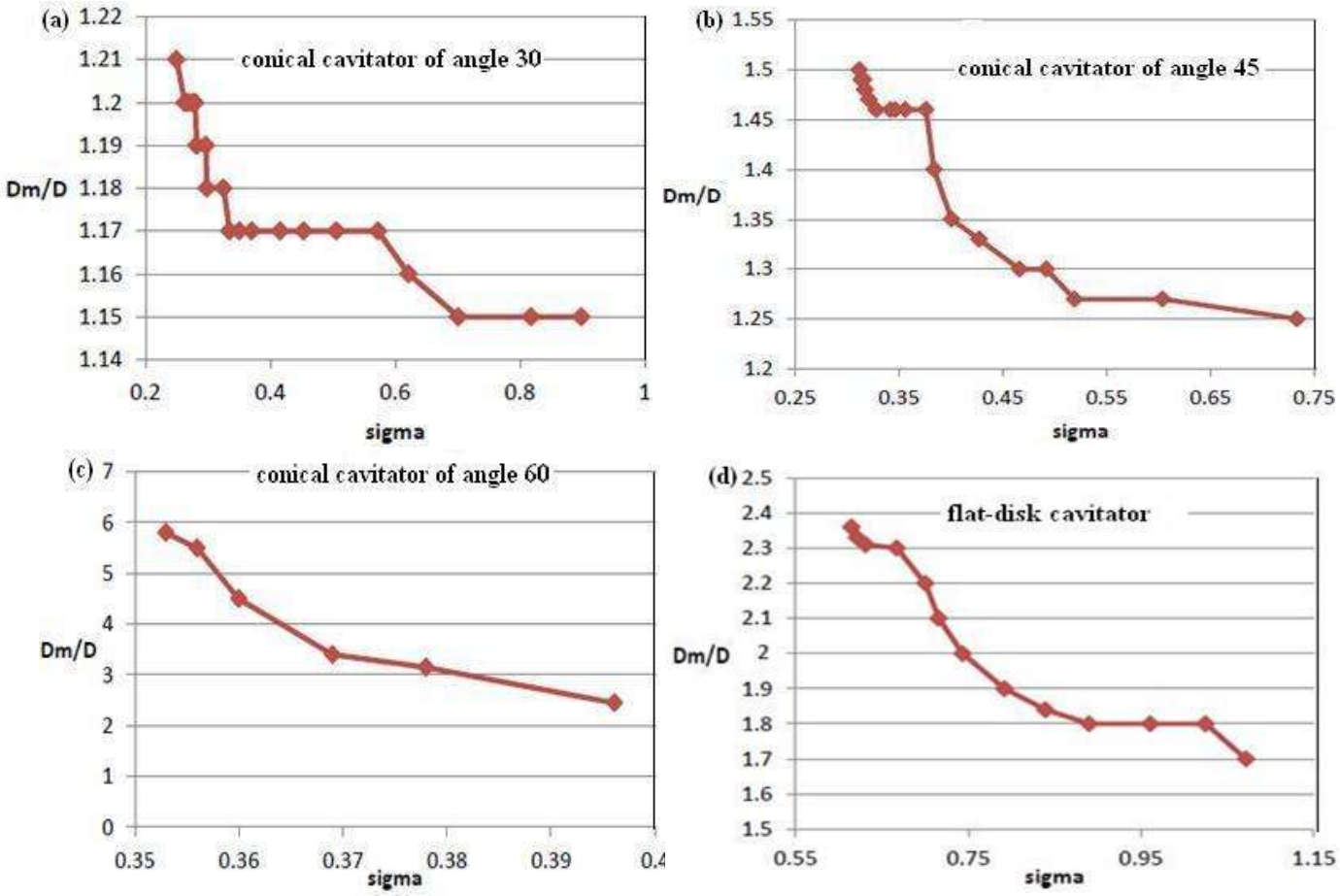

Figs.12. The ratio of maximum diameter of supercavity to the base diameter of different cavitators versus the cavitation number

In Figs.13, the dynamic behavior of supercavity has been represented in the selected sequent frames captured by a high-speed photography system for different cavitators. From them, the geometrical characteristics of supercavity such as its length and diameter are extracted. With gradual decreasing in flow velocity and pressure in the test section, the supercavity length decreases with lapsing of time which results in gradual increasing in skin friction drag force. On the other hand, by gradual decreasing in pressure at the cavitator's tip, the pressure drag force gradually decreases. Therefore, because the pressure drag is dominant compared to skin friction drag, the total drag decreases with lapsing of time. Moreover, due to greater decrease in the dynamic pressure in the test section compared to decrease in drag, the drag coefficient decreases with lapsing of time.

Fig.14 represents that the drag coefficient increases with the cavitation number and the flat disk-shaped cavitator has undesirable hydrodynamic performance in comparison with conical cavitators.

Figs.15 depict the ratio of supercavity's length to its maximum diameter versus the cavitation number for different cavitators. It is seen that the more closeness of cavitation number to the cavitation number of blockage **Error! Reference source not found.**leads to more vertically locating of the points. Also it seems that increase in conical cavitator's angle results in increase in**Error! Reference source not found.**and for the flat disk-shaped cavitator, it is the greatest (**Error! Reference source not found.**). Furthermore, it is comprehended that **Error! Reference source not found.**for the conical cavitators of angles **Error! Reference source not found.** which are respectively 1.78, 2.0, 2.24, are greater than **Error! Reference source not found.** for similar symmetric wedge-shaped cavitators with the chord of C=5 mm situated in a water channel with the height of H=40 mm which are from the following equation 0.374, 0.619, 0.92, respectively [21]:

$$\frac{\sigma_{blockage}}{1+\frac{\sigma_{blockage}}{2}} = \frac{4\gamma}{\pi} cosh^{-1}\left(e^{\pi\frac{C}{H}}\right) \quad (2)$$

By ventilation of supercavity, a greater supercavity length can be achieved. From Fig.16, it is seen that by increasing the volumetric flow rate of injected air into the supercavity and thus by increasing its length, the drag coefficient decreases.

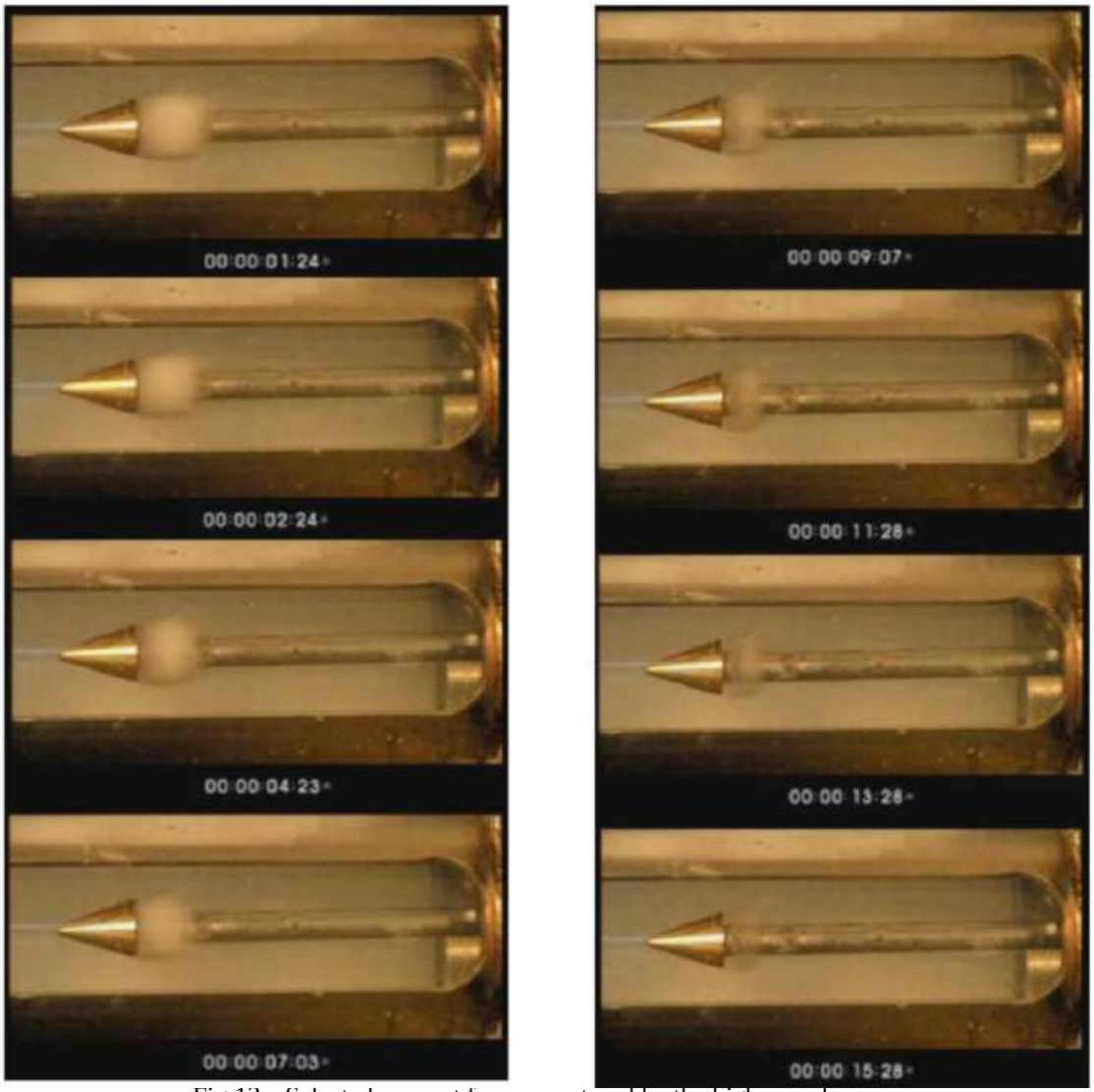

Fig.13a. Selected sequent frames captured by the high-speed camera
for the conical cavitator of angle 30° at the velocity range of 15-24 m/s

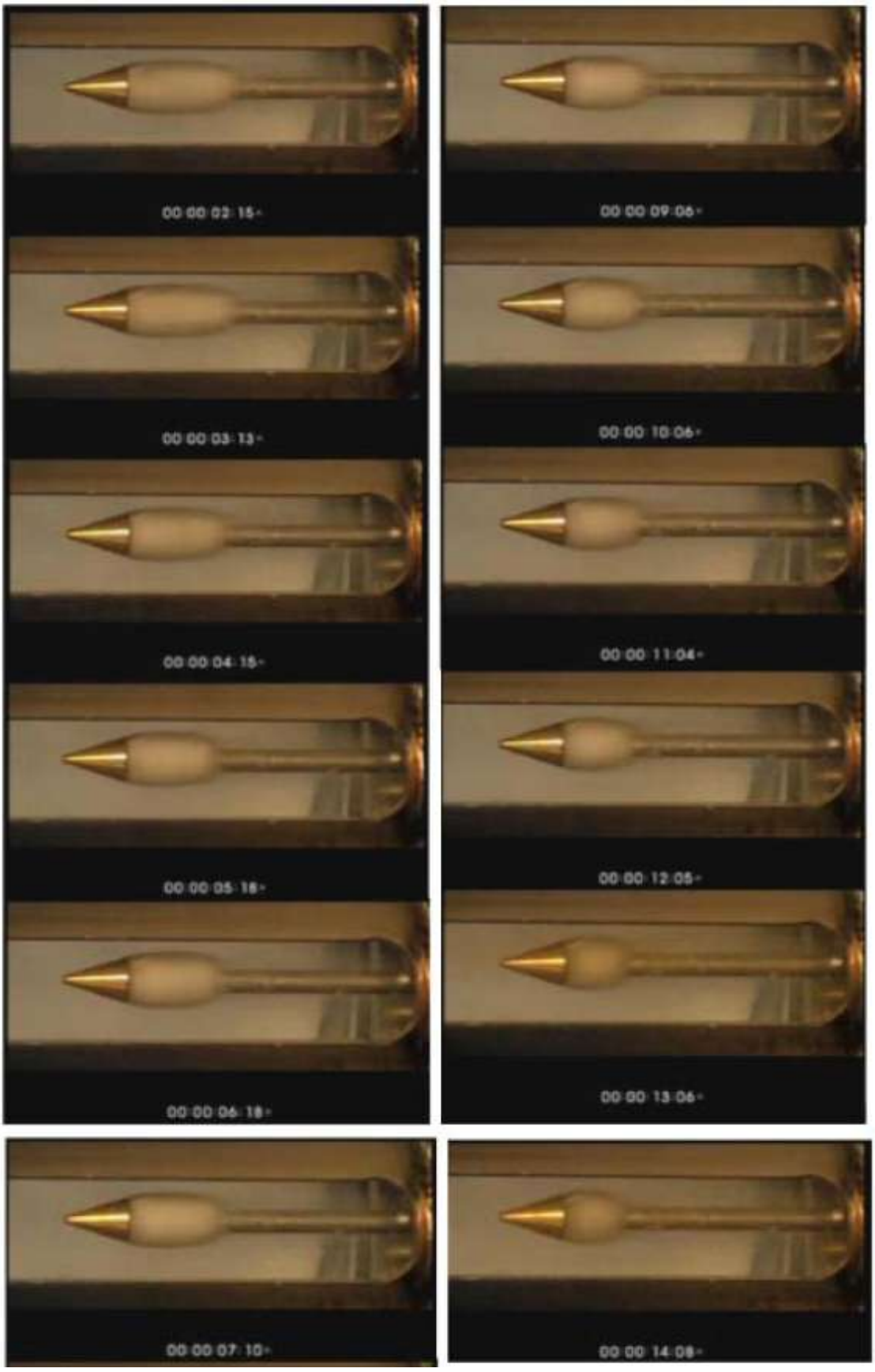

Fig.13b. Selected sequent frames captured by the high-speed camera for the conical cavitator of angle 30° at the velocity range of 25-38 m/s

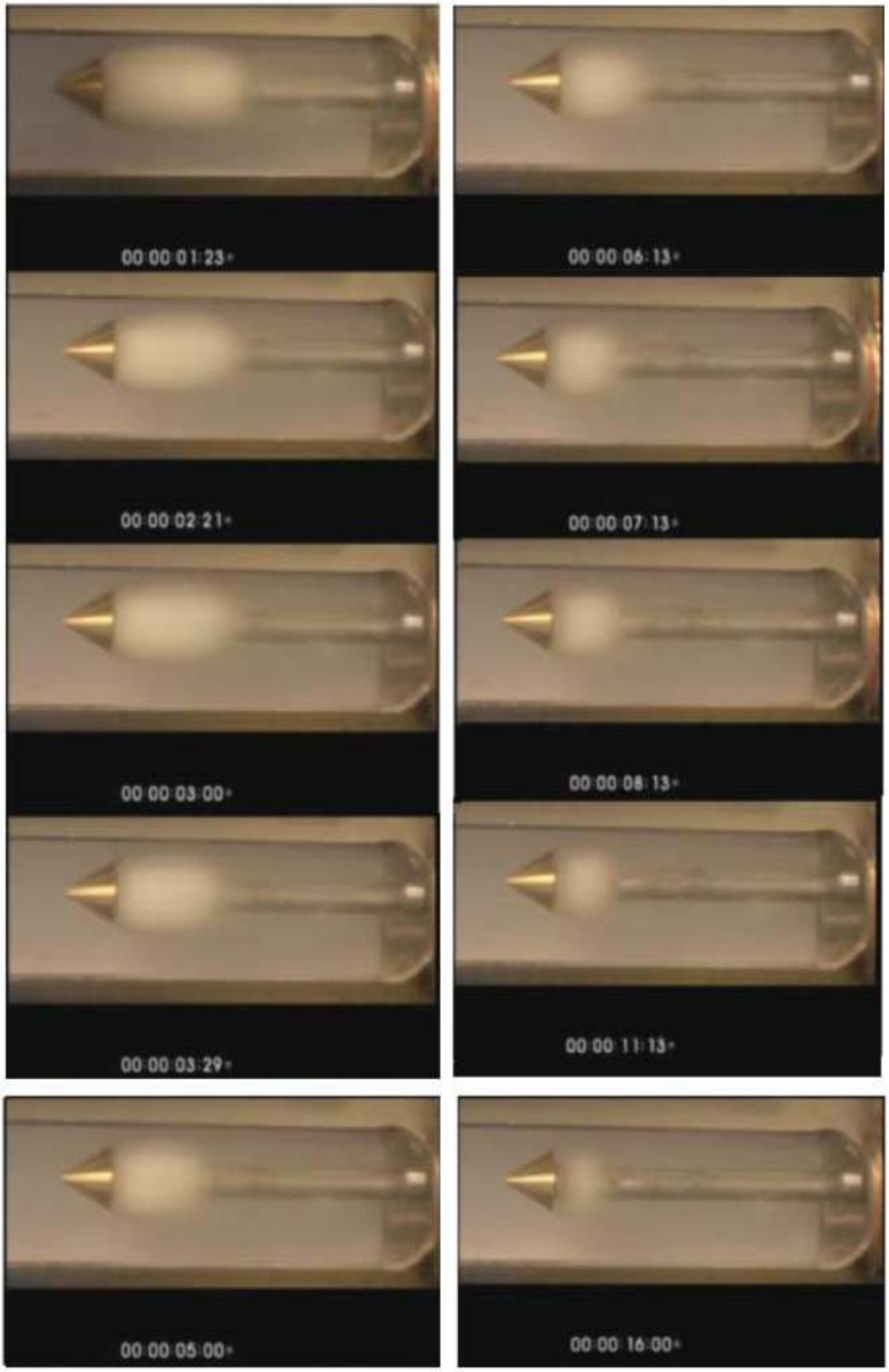

Fig.13c. Selected sequent frames captured by the high-speed camera for the conical cavitator of angle 45° at the velocity range of 16-26 m/s

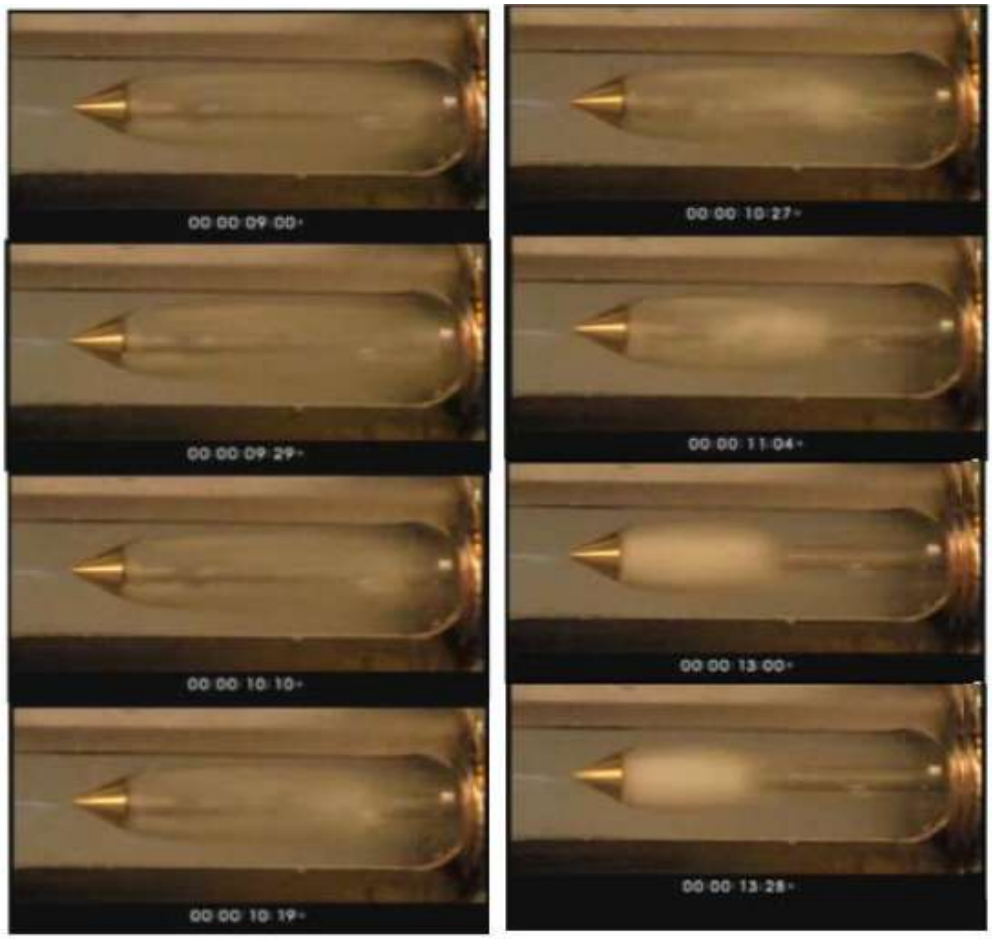

Fig.13d. Selected sequent frames captured by the high-speed camera for the conical cavitator of angle 45° at the velocity range of 27-37 m/s

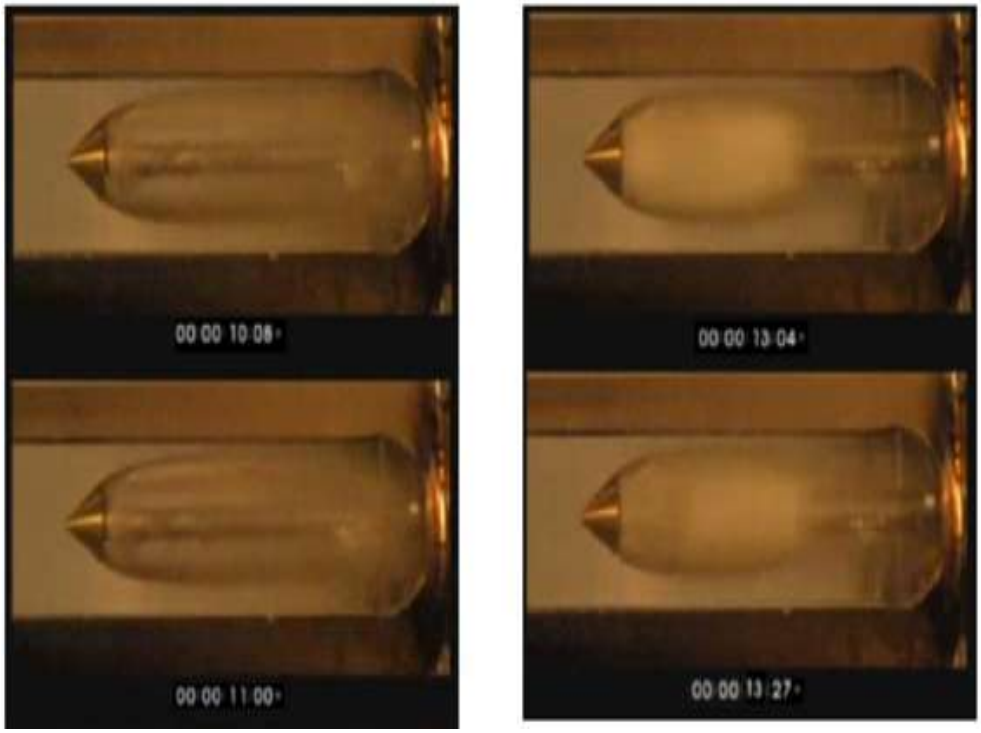

Fig.13e. Selected sequent frames captured by the high-speed camera for the conical cavitator of angle 60° at the velocity range of 26-36 m/s

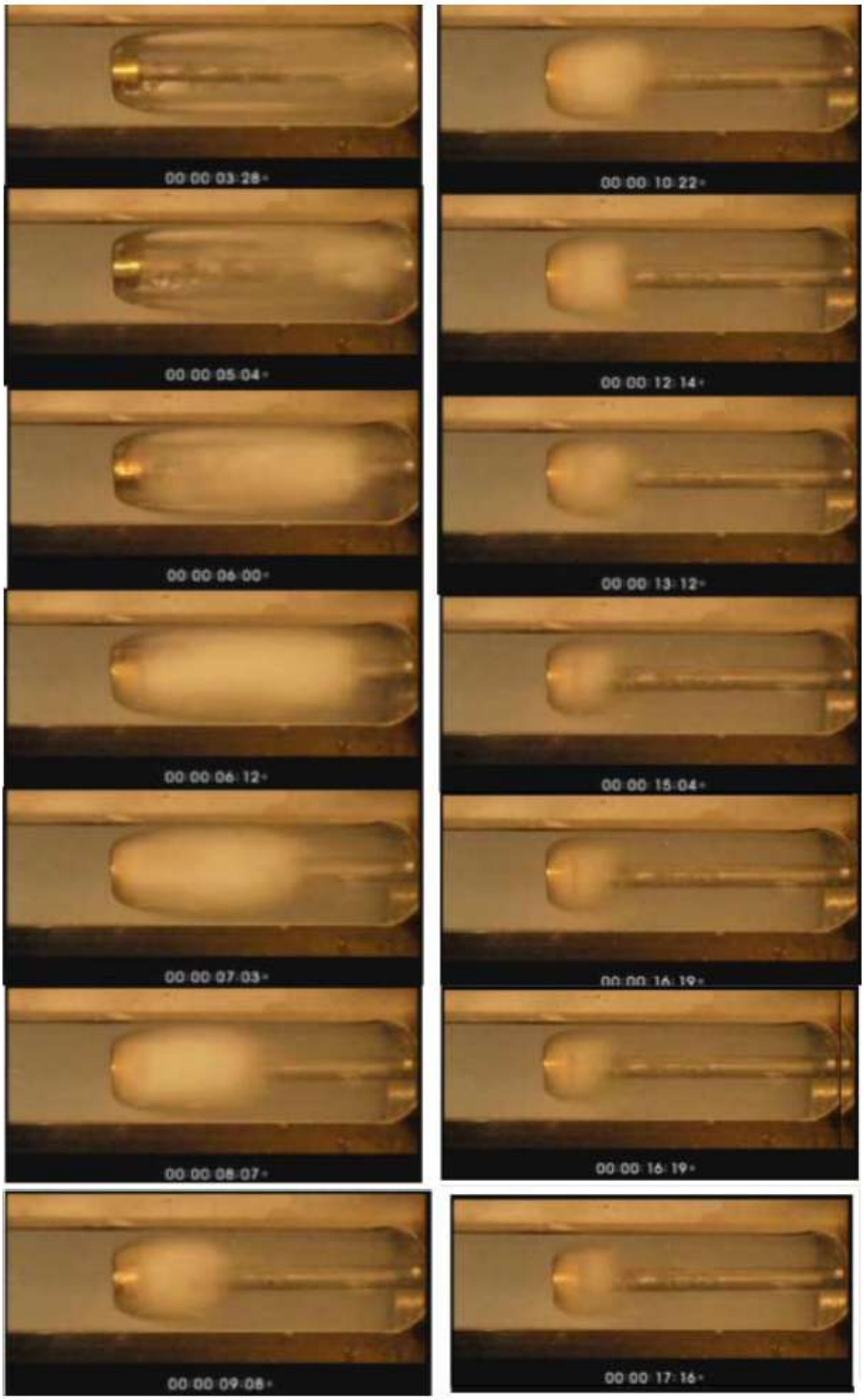

Fig.13f. Selected sequent frames captured by the high-speed camera
For the flat disk-shaped cavitator at the velocity range of 13-20 m/s

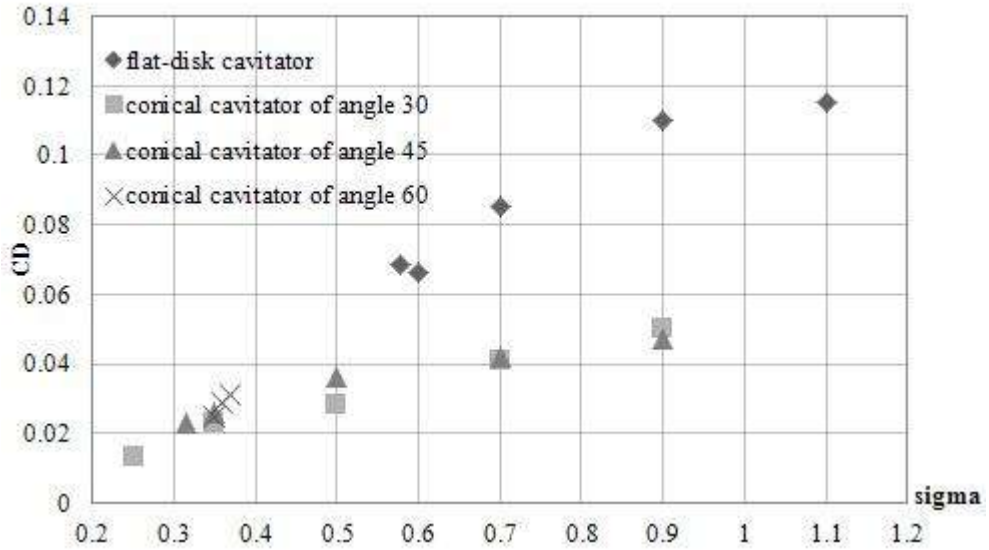

Fig.14. Drag coefficient for different cavitators versus the cavitation number

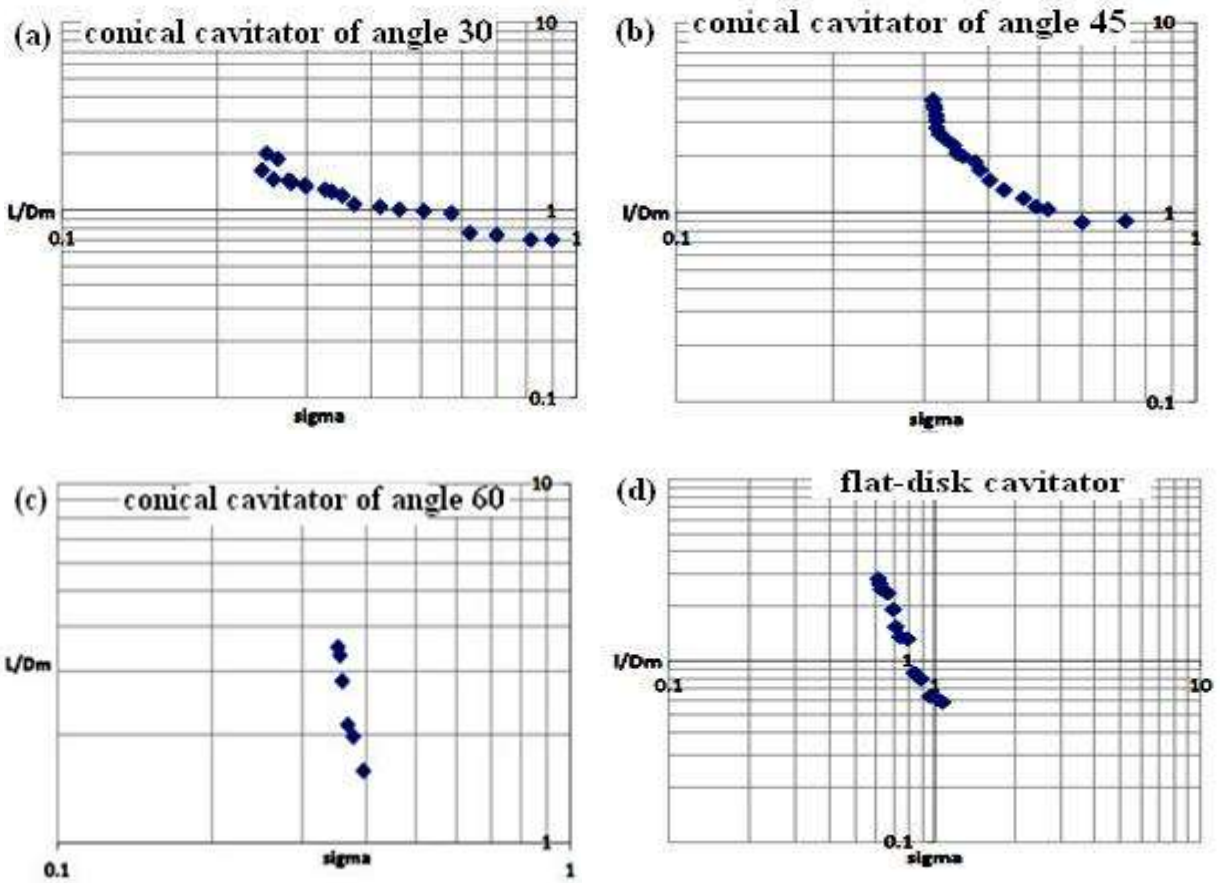

Figs.15. The ratio of supercavity length to its maximum diameter versus the cavitation number for different cavitators in the logarithmic coordinates system

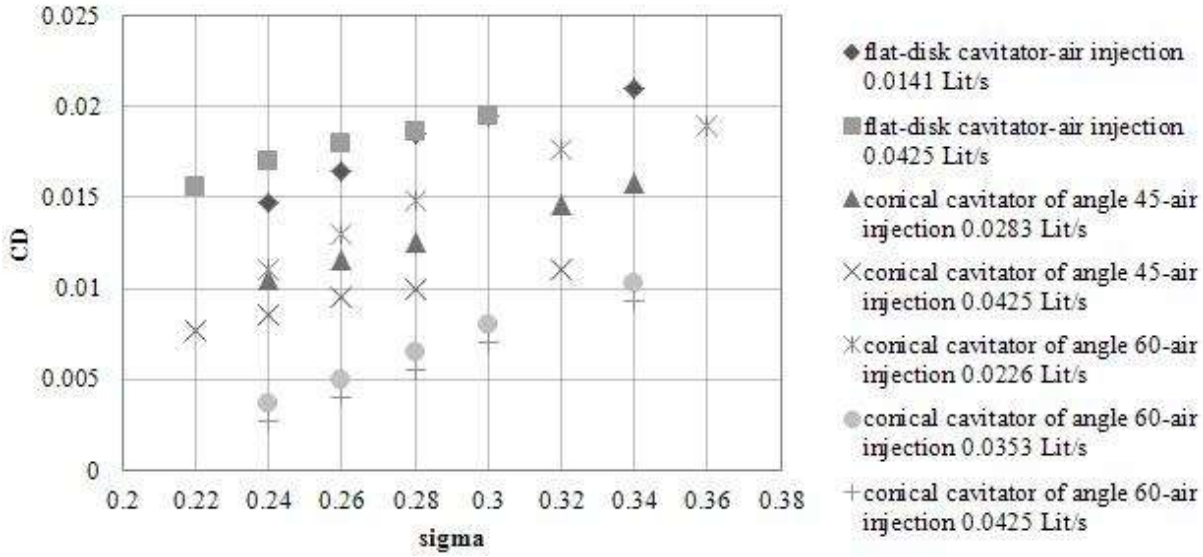

Fig.16. Drag coefficient for different cavitators with different volumetric flow rates of air injection into the supercavity versus the cavitation number

[4] CONCLUSION

In this experimental investigation, the supercavitating flows over a cylindrical body equipped with the conical cavitators of angles 30°,45°,60° and also a flat dick-shaped cavitator inside an open-circuit water tunnel have been studied by using the appropriate calibrated sensors and a high-speed camera to capture the dynamic behavior of supercavity and extract its geometrical characteristics. In experiments, the effects of cavitator, the velocity of flow in the test section and the volumetric flow rate of air injection into the supercavity on its size and also the drag coefficient have been investigated. It was found that the formation of supercavity around the body can decrease the drag. For this purpose, both conical cavitator of angle 60° and the flat disk-shaped cavitator because of their serious role in the blockage are not recommended. The ventilation of the supercavity which elongates the supercavity leads to decrease in the drag more. For example, in the supercavitating flow with the velocity of 34 m/s over the model with the conical cavitator of 45°, the air injection with the volumetric flow rate of 0.0283 lit/s into the supercavity causes 6% decrease in the drag and by increasing the flow rate of ventilation to 0.0425 lit/s, 19% decrease in the drag can be achieved. At the same flow velocity and for the conical cavitator of angle 60°, for air injections of 0.0226, 0.0353, 0.0425 lit/s, the decreases in the drag are respectively 7%, 15%, 21% and for the flat disk-shaped cavitator with the ventilation rate of 0.0141 and 0.0425 lit/s, the decreases in the drag respectively equals 18% and 21%. Altogether, the results of this study illustrated that the application of cavitators can result in a considerable decrease in the drag force on underwater vehicles such as submarines and consequently enhance their hydrodynamic performance.

REFERENCES

[5] J. Y. Choi and M. Ruzzene, "Stability analysis of supercavitating underwater vehicles with adaptive cavitator", Int. J. Mech. Sci., vol. 48, pp. 1360-1370, 2006.

[6] Ch. Hu, H. L. Yang, C. B. Zhao and W. H. Huang, "Unsteady supercavitating flow past cones", J. Hydrodyn., vol. 18, no. 3, pp. 262-272, 2006.

[7] Ch. Ma, D. Jia, Zh. F. Qian and D. H. Feng, "Study on cavitation flows of underwater vehicle", Conference of Global Chinese Scholars on Hydrodynamics, pp. 373-377, 2006.

[8] E. Amromin, "Analysis of body supercavitation in shallow water", Ocean Eng., vol. 34, pp. 1602-1606, 2007.

[9] R. Shafaghat, S. M. Hosseinalipou, N. M. Nouri and I. Lashgari, "Shape optimization of two-dimensional cavitators in supercavitating flows, using NSGA II algorithm", Appl. Ocean Res., vol. 30, pp. 305-310, 2008.

[10] R. Shafagat, S. M. Hosseinalipour, N. M. Nouri and A. Vahedgermi, "Mathematical approach to investigate the behavior of the principal parameters in axisymmetric supercavitating flows, using boundary element method", J. Mech., vol. 25, no. 4, pp. 65-73, 2009.

[11] R. Shafaghat, S. M. Hosseinalipour, I. Lashgari and A. Vahedgermi, "Shape optimization of axisymmetric cavitators in supercavitating flows, using the NSGA II algorithm", Appl. Ocean Res., vol. 33, pp. 193-198, 2011.

[12] Z. M. Hu, H. S. Dou and B. C. Khoo, "On the modified dispersion-controlled dissipative (DCD) scheme for computation of flow supercavitation", Comput. Fluids, vol. 40, pp. 315-323, 2011.

[13] S. Park and Sh. H. Rhee, "Computational analysis of turbulent supercavitating flow around a two-dimensional wedge-shaped cavitator geometry", Comput. Fluids, vol. 70, pp. 73-85, 2012.

[14] E. Roohi, A. P. Zahiri and M. Passandideh-Fard, "Numerical simulation of cavitation around a two-dimensional hydrofoil using VOF method and LES turbulence model", Appl. Math. Model, vol. 37, pp. 6469-6488, 2013.

[15] Zh. Shang, "Numerical investigations of supercavitation around blunt bodies of submarine shape", Appl. Math. Model, vol. 37, no. 20, pp. 8836-8845, 2013.

[16] B. Saranjam, "Experimental and numerical investigation of an unsteady supercavitating moving body", Ocean Eng., vol. 59, pp. 9-14, 2013.

[17] M. R. Pendar and E. Roohi, "Investigation of cavitation around 3D hemispherical head-form body and conical cavitators using different turbulence and cavitation models", Ocean Eng., vol. 112, pp. 287-306, 2016.

[18] R. B. Thorpe, G. M. Evans and K. Zhang, "Liquid recirculation and bubble breakup beneath ventilated gas cavities", Chem. Eng. Sci., vol. 56, pp. 6399-6409, 2001.

[19] X. M. Feng, Ch. J. Lu and T. Q. Hu, "Experimental research on a supercavitating slender body of revolution with ventilation", J. Hydrodyn., vol. 14, no. 2, pp. 17-23, 2002.

[20] L. P. Jia, C. Wang, Y. J. Wei, H. B. Wang, J. Z. Zhang and K. P. Yu, "Numerical simulation of artificial ventilated cavity", J. Hydrodyn., vol. 18, no. 3, pp. 273-279, 2006.

[21] X. W. Zhang, Y. J. Wei, J. ZH. Zhang, C. Wang and K. P. Yu, "Experimental research on the shape characters of natural and ventilated supercavitation", J. Hydrodyn., vol. 19, no. 5, pp. 564-571, 2007.

[22] X. Chen, C. J. Lu, J. Li and Z. C. Pan, "The wall effect on ventilated cavitating flows in closed cavitation tunnels", J. Hydrodyn., vol. 20, no. 5, pp. 561-566, 2008.
[23] J. J. Zhou, K. P. Yu, M. Yang and X. H. Wan, "On the gas leakage way of supercavity and vehicle vibration", J. Hydrodyn., vol. 22, no. 5, pp. 866-871, 2010.
[24] N. M. Nouri, M. Riahi, A. Valipour, M. M. Raeyatpishe and E. Molavi, "Analytical and experimental study of hydrodynamic and hydroacoustic effects of air injection flow rate in ventilated supercavitation", Ocean Eng., vol. 95, pp. 94-105, 2015.
[25] J. P. Franc and J. M. Michel, "Fundamentals of Cavitation" Kluwer Academic Publishers, Kluwer, 2004.